STABLIZATION AND TRACKING CONTROL OF CHAOS IN A PERMANENT MAGNET SYNCHRONOUS MOTOR MODEL

Le Hoa Nguyen*

The University of Danang – University of Science and Technology, Vietnam

*Corresponding author: nglehoa@dut.udn.vn

(Received: May 15, 2025; Revised: June 11, 2025; Accepted: June 19, 2025)

DOI: 10.31130/ud-jst.2025.23(9B).515E

Abstract – In this paper, the problem of controlling chaos in a permanent magnet synchronous motor (PMSM) is addressed. First, the chaotic dynamics of a PMSM model are presented where the bifurcation diagram and the largest Lyapunov exponent techniques are used to explore chaos. Then, novel and efficient control laws based on the general input-state linearization control technique are proposed for stabilization and tracking control of the chaotic PMSM model. The proposed control laws use the direct- and quadrature-axis stator voltage components as controlled variables; therefore, they are convenient to implement in real applications. Numerical simulations are performed to demonstrate and verify the effectiveness of the proposed control methods.

Key words – Permanent magnet synchronous motor; chaotic dynamics; chaos control; input-state linearization technique.

1. Introduction

Over the past decades, the study of chaos has been conducted over a wide range of scientific disciplines such as physics, chemistry, biology, ecology, and others. The occurrence of chaos in motor drive systems was first investigated in the late 1980s [1, 2]. Since then, many studies have reported the presence of chaos in DC drive systems [3, 4], AC drive systems [5-7], and switched reluctance drive systems [8]. A permanent magnet synchronous motor (PMSM) was shown to exhibit bifurcation and chaotic behavior for a certain range of its parameters [9-10]. When a PMSM enters chaos, the motor torque and speed oscillate unpredictably which can cause serious issues in the drive system. To address this problem, various control techniques have been proposed to suppress chaotic oscillations. A nonlinear backstepping control law was proposed by Harb [11] to stabilize the chaotic PMSM model, with the simulation results compared to those obtained using the nonlinear sliding mode control law. Fixed-time adaptive control methods have been proposed to ensure system stabilization within a pre-defined time frame, regardless of initial conditions [12]. Lyapunov-based model predictive control (LMPC) has also been effectively applied in networked environments with data loss, maintaining system performance through predictive compensation [13]. Additionally, adaptive terminal sliding mode controllers have demonstrated robust performance in chaotic PMSMs under uncertainties and disturbances [14]. Ataei et al. [15] and Zribi et al. [16] introduced different control laws for the chaotic PMSM model to achieve negative Lyapunov exponents in the closed loop control system, thereby eliminating chaos. To handle the uncertainties in system parameters and disturbances in external load torque, adaptive robust control methods have been proposed [17, 18]. Another approach to suppress chaos in the PMSM model is to introduce mutual correlation among system variables. By selecting the proper correlation factor, the controlled PMSM system is driven from the chaotic state to a the stable state [19].

In this paper, both stabilization and tracking control laws for the chaotic PMSM model are proposed using the general input-state linearization control technique. The objective of the stabilization control is to drive inherent chaotic PMSM orbits asymptotically toward the origin. In the tracking control, the angular speed of the PMSM model is required to follow the desired speed while the other system states remain asymptotically stable. The advantage of the proposed control laws over previous methods is that they use the direct and quadrature-axis stator voltage components as the controlled variables, making them convenient to implement in real applications.

2. Mathematical model of PMSMs

The mathematical model of PMSM on the *d-q* axis is described as follows [10].

$$\begin{cases} \dfrac{d\bar{i}_d}{d\bar{t}} = \dfrac{1}{L_d}\left(\bar{u}_d - R\bar{i}_d + \bar{\omega}L_q\bar{i}_q\right), \\ \dfrac{d\bar{i}_q}{d\bar{t}} = \dfrac{1}{L_q}\left(\bar{u}_q - R\bar{i}_q - \bar{\omega}L_d\bar{i}_d + \bar{\omega}\psi_r\right), \\ \dfrac{d\bar{\omega}}{d\bar{t}} = \dfrac{1}{J}\left[n_p\psi_r\bar{i}_q + n_p\left(L_d - L_q\right)\bar{i}_d\bar{i}_q - \bar{T}_L - \beta\bar{\omega}\right]. \end{cases} \quad (1)$$

where, $\bar{\omega}$ (rad/s) is the angular speed of the motor; $\bar{i}_d$ (A) and $\bar{i}_q$ (A), respectively, are the direct and quadrature stator current components; $\bar{u}_d$ (V) and $\bar{u}_q$ (V), respectively, are the direct and quadrature stator voltage components; $\bar{T}_L$ (Nm) is the load torque; J (Kgm^2) is the polar moment of inertia; L_d (mH) and L_q (mH), are the direct and quadrature stator inductors, respectively; R (Ω) is the winding resistance of the stator; ψ_r (Wb) is the permanent magnet flux; β (Nrad^{-1}s) is the viscous damping coefficient, and n_p is the number of pole-pair.

According to [10], by using the following transformation:

$$\begin{cases} \bar{\mathbf{x}} = \boldsymbol{\Gamma}\mathbf{x}, \\ \bar{t} = \tau t. \end{cases} \quad (2)$$

where:

$$\bar{\mathbf{x}} = \begin{bmatrix} \bar{i}_d & \bar{i}_q & \bar{\omega} \end{bmatrix}^T, \qquad \mathbf{x} = \begin{bmatrix} i_d & i_q & \omega \end{bmatrix}^T,$$

$$\boldsymbol{\Gamma} = \begin{bmatrix} b\kappa & 0 & 0 \\ 0 & \kappa & 0 \\ 0 & 0 & 1/\tau \end{bmatrix} \quad b = \frac{L_q}{L_d}, \ \kappa = \frac{\beta}{n_p \tau \psi_r}, \ \tau = \frac{L_q}{R}.$$

and with assumption that the PMSM has a smooth-air-gap (i.e., $L_d = L_q = L$), the following dimensionless form of the PMSM model is obtained:

$$\begin{cases} \dfrac{di_d}{dt} = -i_d + i_q\omega + u_d, \\ \dfrac{di_q}{dt} = -i_q - i_d\omega + \mu\omega + u_q, \\ \dfrac{d\omega}{dt} = \sigma\left(i_q - \omega\right) - T_L. \end{cases} \tag{3}$$

in which, parameters of (3) are given by

$$\mu = \frac{n_p\psi_r^2}{R\beta}, \quad \sigma = \frac{L_q\beta}{RJ}, \quad u_d = \frac{n_p\psi_r L_q}{\beta R^2}\bar{u}_d, \quad u_q = \frac{n_p\psi_r L_q}{\beta R^2}\bar{u}_q$$

and $T_L = \dfrac{L_q^2}{JR^2}\bar{T}_L$.

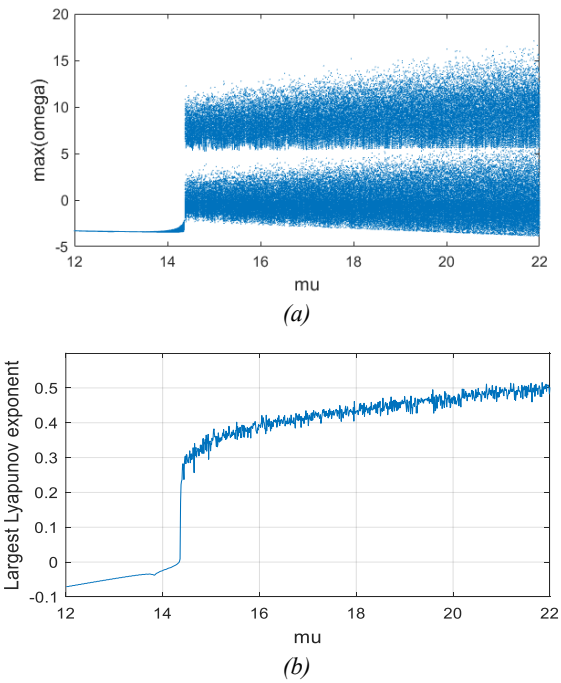

Figure 1. *a) The bifurcation diagram showing all the peak values of w corresponding to the variation of the bifurcation parameter u; and b) the corresponding variation of the largest Lyapunov exponent of the unforced PMSM model [10]*

The nonlinear dynamic behaviors of (3) have been investigated in [10-12]. The results have shown that in the case of the unforced system (i.e., $u_d = u_q = 0$ and $T_L = 0$), and if the values of μ and σ are within a certain range, PMSM exhibits chaotic oscillation. It is noted that all simulation results presented in this paper were obtained using Matlab software. The bifurcation diagram which shows all peaks generated by (3) for a given value of the bifurcation parameter, μ is shown in Figure 1(a). Additionally, the largest Lyapunov exponent corresponding to each value of the bifurcation parameter is caculated and the obtained result is shown in Figure 1(b). In these simulations, σ is set to 5.46. It is obvious that the PMSM model enters chaotic oscillations (as indicated by a positive value of the Lyapunov exponent) for $\mu > 14.3$. The chaotic attractor and time series of the state variables that display the chaotic behavior of the PMSM model for $\mu = 20$ are shown in Figure 2.

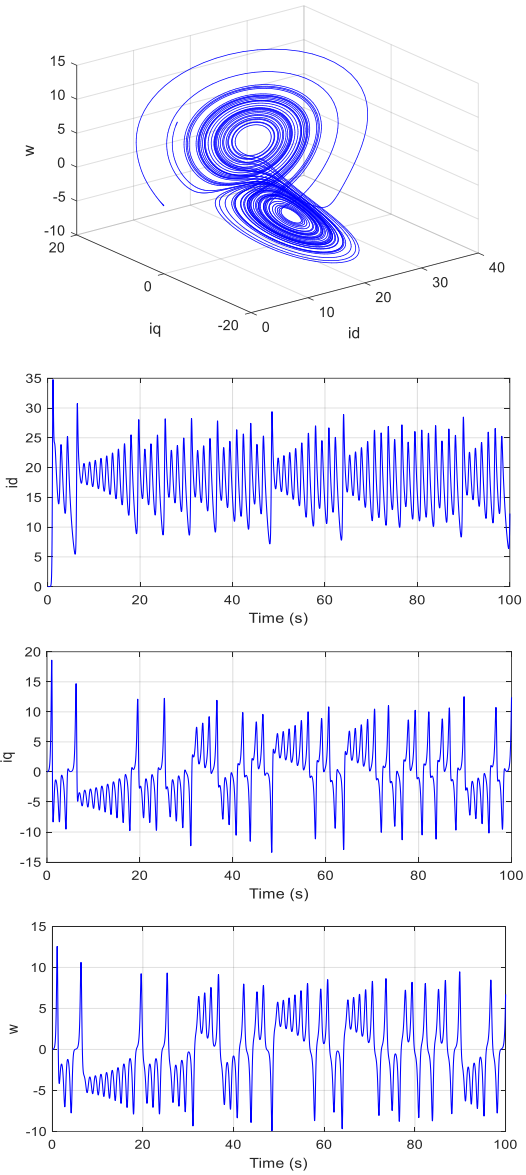

Figure 2. *PMSM exhibits chaotic behavior for μ = 20 and σ = 5.46: Phase portrait (top figure) and time series of the state variables (three bottom figures)*

3. Control of chaos in PMSMs

3.1. Input-state linearization control technique

Consider the class of nonlinear systems of the form

$$\dot{\mathbf{x}} = \mathbf{A}\mathbf{x} + \mathbf{B}\gamma(\mathbf{x})\left(\mathbf{u} - \boldsymbol{\alpha}(\mathbf{x})\right), \tag{4}$$

where $\mathbf{u}$ is the control input, $\gamma: D \subset R^n \to R$ and $\gamma \neq 0, \forall \mathbf{x} \in D$, and the pair $(\mathbf{A}, \mathbf{B})$ is controllable. Then, we can choose the control law as follows [20].

$$\mathbf{u} = \boldsymbol{\alpha}(\mathbf{x}) + \beta(\mathbf{x})\mathbf{v}, \tag{5}$$

where $\beta(\mathbf{x}) = \dfrac{1}{\gamma(\mathbf{x})}$. That leads the closed-loop control system to become:

$$\dot{\mathbf{x}} = \mathbf{A}\mathbf{x} + \mathbf{B}\mathbf{v}. \tag{6}$$

Since, the system in (6) is linear time-invariant, one can design control law $\mathbf{v}$ to stabilize or to impose the system to any desirable performance.

3.2. Chaos suppression

In Section 2, it has been clearly shown that the unforced PMSM model (i.e., with $u_d = u_q = T_L = 0$) displays chaotic behavior which corresponds to the system being unstable at the equilibrium point. Therefore, to eliminate undesirable chaotic oscillations, the control law is designed so that the closed loop control system is asymptotically stable at the equilibrium point. Furthermore, to increase the feasibility of the designed control system, the control law must use the direct and quadrature stator voltages u_d and u_q, as manipulated variables. To this end, the state variables (i_d, i_q, ω) are assumed to be available for access.

It can be seen that the system described in (3) can be written in the form of (4), where

$$\mathbf{x} = \begin{bmatrix} i_d \\ i_q \\ \omega \end{bmatrix}, \mathbf{u} = \begin{bmatrix} v_d \\ v_q \end{bmatrix}, \mathbf{A} = \begin{bmatrix} -1 & 0 & 0 \\ 0 & -1 & \mu \\ 0 & \sigma & -\sigma \end{bmatrix}, \mathbf{B} = \begin{bmatrix} 1 & 0 \\ 0 & 1 \\ 0 & 0 \end{bmatrix},$$

$$\gamma(\mathbf{x}) = 1, \text{ and } \boldsymbol{\alpha}(\mathbf{x}) = \begin{bmatrix} -i_q\omega \\ i_d\omega \end{bmatrix}. \tag{7}$$

According to (5), the control law then is chosen as

$$\mathbf{u} = \begin{bmatrix} u_d \\ u_q \end{bmatrix} = \begin{bmatrix} -i_q\omega + v_d \\ i_d\omega + v_q \end{bmatrix} \tag{8}$$

The closed loop control system leads to

$$\dot{\mathbf{x}} = \mathbf{A}\mathbf{x} + \mathbf{B}\mathbf{v}, \text{ where } v = \begin{bmatrix} v_d \\ v_q \end{bmatrix}. \tag{9}$$

To stabilize the linear system in (9), the state feedback control law is chosen as

$$\mathbf{v} = -\mathbf{K}\mathbf{x} = -\begin{bmatrix} k_1 & k_2 & k_3 \\ k_4 & k_5 & k_6 \end{bmatrix}\begin{bmatrix} i_d \\ i_q \\ \omega \end{bmatrix}. \tag{10}$$

Substitute (10) into (9), we have

$$\dot{\mathbf{x}} = (\mathbf{A} - \mathbf{B}\mathbf{K})\mathbf{x}, \tag{11}$$

where,

$$\mathbf{A} - \mathbf{B}\mathbf{K} = \begin{bmatrix} -1-k_1 & -k_2 & -k_3 \\ -k_4 & -1-k_5 & \mu - k_6 \\ 0 & \sigma & -\sigma \end{bmatrix}. \tag{12}$$

It is obviously that, the system described in (9) with the control law in (10) is asymptotically stable if the matrix $\mathbf{A} - \mathbf{B}\mathbf{K}$ is Hurwitz. Therefore, the gain matrix $\mathbf{K}$ can be found as follows:

We have,

$$\begin{aligned} &\det(\lambda\mathbf{I} - (\mathbf{A} - \mathbf{B}\mathbf{K})) = \\ &= \det\left(\begin{bmatrix} \lambda + 1 + k_1 & k_2 & k_3 \\ k_4 & \lambda + 1 + k_5 & -\mu + k_6 \\ 0 & -\sigma & \sigma \end{bmatrix}\right) \\ &= \lambda^3 + a_2\lambda^2 + a_1\lambda + a_0 \end{aligned} \tag{13}$$

where,

$$a_0 = \sigma\left(1 - \mu + (1-\mu)k_1 + k_5 + k_6 + k_1k_5 + k_1k_6 - k_2k_4 - k_3k_4\right),$$

$$a_1 = 1 + 2\sigma - \mu\sigma + (1+\sigma)k_1 + (1+\sigma)k_5 + \sigma k_6 + k_1k_5 - k_2k_4,$$

$$a_2 = 2 + \sigma + k_1 + k_5.$$

According to Routh-Hurwitz stability criterion, to guarantee the closed loop system in (11) to be asymptotically stable, $k_i, i = \overline{1, 6}$ are selected such that the following inequalities hold.

$$\begin{aligned} &a_i > 0, \qquad i = 0, 1, 2 \\ &a_1a_2 - a_0 > 0 \end{aligned} \tag{14}$$

However, in order to achieve the desired performance (e.g., speed of response, overshoot, control effort, robustness, etc.) various techniques can be applied to design the gain matrix $\mathbf{K}$ such as direct pole placement, Ackermann's formular or linear quadratic regulator (LQR).

Combining (8) and (10), finally, the control signals are given by

$$\begin{aligned} u_d &= -i_q\omega - k_1i_d - k_2i_q - k_3\omega, \\ u_q &= i_d\omega - k_4i_d - k_5i_q - k_6\omega. \end{aligned} \tag{15}$$

To verify the effectiveness of the proposed control laws in (15), a simulation is conducted for the cases when $\mu = 20$ and $\sigma = 5.46$. In this simulation, the control gains $k_i, i = \overline{1, 6}$ are designed using the pole placement technique to ensure fast convergence (i.e., short settling time) and minimal overshoot in the system's response. Specifically, three desired poles of the closed loop system (11) are selected as: $\lambda_1 = -10$, $\lambda_{2,3} = -5 \pm j2$. The first pole, with a large negative real part, contributes the rapid decay of the transient response, while the other two poles, which have small imaginary parts, introduce slight oscilatory behavior, resulting in a small overshoot. Finally, by using the *place* function in Matlab, the control gains are obtained as follows: $k_1 = 9$, $k_2 = 0$, $k_3 = 0$, $k_4 = 0$, $k_5 = 3.54$, and $k_6 = 20.7714$. To eliminate the effect of the initial states, the control laws are applied to the system at t = 20 s, the system state time courses are shown in Figure 3. It can be seen from Figure 3 that the system states settle to a stable equilibrium quickly.

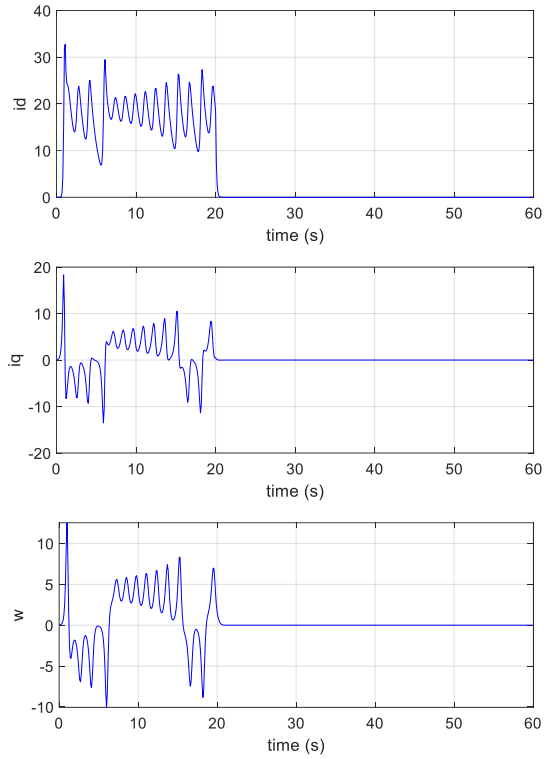

Figure 3. *Time series of the state variables (i_d, i_q, ω), which initially exhibit chaotic oscillations, quickly settle to the origin when the control laws in (15) are applied at t = 20 s*

3.3. Tracking control

For the tracking control, the objective is to design the control signals u_d and u_q such that the chaotic oscillations are damped out while forcing the angular speed to a constant desired value $\hat{\omega}$. At $\omega = \hat{\omega}$, the system is in the steady state (i.e., $\frac{d\omega}{dt} = 0$, $\frac{di_d}{dt} = 0$, $\frac{di_q}{dt} = 0$), therefore, from (3) we obtain the desired values $\hat{i}_d$, $\hat{i}_q$, as well as the required steady state control signals $\hat{u}_d$ and $\hat{u}_q$ that satisfy.

$$\begin{cases} 0 = -\hat{i}_d + \hat{i}_q\hat{\omega} + \hat{u}_d, \\ 0 = -\hat{i}_q - \hat{i}_d\hat{\omega} + \mu\hat{\omega} + \hat{u}_q, \\ 0 = \sigma\left(\hat{i}_q - \hat{\omega}\right). \end{cases} \tag{16}$$

By setting $\hat{u}_d = 0$, finally we have

$$\hat{i}_d = \hat{\omega}^2, \quad \hat{i}_q = \hat{\omega}, \quad \hat{u}_q = \left(1-\mu\right)\hat{\omega} + \hat{\omega}^3. \tag{17}$$

Define the following errors

$$e_{id} = i_d - \hat{i}_d, \quad e_{iq} = i_q - \hat{i}_q, \quad e_\omega = \omega - \hat{\omega}. \tag{18}$$

and change the control signals to

$$v_d = u_d - \hat{u}_d, \quad v_q = u_q - \hat{u}_q. \tag{19}$$

Then, we obtain the error dynamics as

$$\begin{cases} \dot{e}_{id} = -e_{id} + \hat{\omega}e_{iq} + \hat{i}_q e_\omega + e_{iq}e_\omega + v_d, \\ \dot{e}_{iq} = -\hat{\omega}e_{id} - e_{iq} + \left(\mu - \hat{i}_d\right)e_3 - e_{id}e_\omega + v_q, \\ \dot{e}_\omega = \sigma\left(e_{iq} - e_\omega\right). \end{cases} \tag{20}$$

It can be seen that the nonlinear system described in (20) has an equilibrium point at the origin when $v_d = v_q = 0$. The control problem leads to the design control signals v_d and v_q such that the system in (20) is asymptotically stable at the origin.

It is also clearly that (20) can be written in the form of (4) as

$$\dot{\bar{\mathbf{x}}} = \bar{\mathbf{A}}\bar{\mathbf{x}} + \bar{\mathbf{B}}\bar{\gamma}(\bar{\mathbf{x}})\left(\bar{\mathbf{v}} - \bar{\boldsymbol{\alpha}}(\bar{\mathbf{x}})\right). \tag{21}$$

where,

$$\bar{\mathbf{x}} = \begin{bmatrix} e_{id} \\ e_{iq} \\ e_\omega \end{bmatrix}, \bar{\mathbf{v}} = \begin{bmatrix} v_d \\ v_q \end{bmatrix}, \bar{\mathbf{A}} = \begin{bmatrix} -1 & \hat{\omega} & \hat{i}_q \\ -\hat{\omega} & -1 & \mu - \hat{i}_d \\ 0 & \sigma & -\sigma \end{bmatrix}, \bar{\mathbf{B}} = \begin{bmatrix} 1 & 0 \\ 0 & 1 \\ 0 & 0 \end{bmatrix},$$

$$\bar{\gamma}(\bar{\mathbf{x}}) = 1, \text{ and } \bar{\boldsymbol{\alpha}}(\bar{\mathbf{x}}) = \begin{bmatrix} -e_{iq}e_\omega \\ e_{id}e_\omega \end{bmatrix}. \tag{22}$$

Following (5), the control law is obtained as

$$\bar{\mathbf{v}} = \begin{bmatrix} v_d \\ v_q \end{bmatrix} = \begin{bmatrix} -e_{iq}e_\omega + w_d \\ e_{id}e_\omega + w_q \end{bmatrix}. \tag{23}$$

The closed-loop control system then becomes

$$\dot{\bar{\mathbf{x}}} = \bar{\mathbf{A}}\bar{\mathbf{x}} + \bar{\mathbf{B}}\bar{\mathbf{w}}, \text{ where } \bar{\mathbf{w}} = \begin{bmatrix} w_d \\ w_q \end{bmatrix}. \tag{24}$$

Similar to (10), the state feedback control law is proposed to stabilize the system in (24) at the origin.

$$\bar{\mathbf{w}} = -\bar{\mathbf{K}}\bar{\mathbf{x}} = -\begin{bmatrix} \bar{k}_1 & \bar{k}_2 & \bar{k}_3 \\ \bar{k}_4 & \bar{k}_5 & \bar{k}_6 \end{bmatrix}\begin{bmatrix} e_{id} \\ e_{iq} \\ e_\omega \end{bmatrix}. \tag{25}$$

Substitute (25) into (24), we have

$$\dot{\bar{\mathbf{x}}} = \left(\bar{\mathbf{A}} - \bar{\mathbf{B}}\bar{\mathbf{K}}\right)\bar{\mathbf{x}}. \tag{26}$$

The gain matrix $\bar{\mathbf{K}}$ is chosen such that the matrix $\bar{\mathbf{A}} - \bar{\mathbf{B}}\bar{\mathbf{K}}$ is Hurwitz. The procedure to find $\bar{k}_i, i = \overline{1,6}$ is similar to that mentioned in (13) and (14).

Finally, by considering (18), (19), (23), and (25), the following control signals are finally obtained

$$\begin{aligned} u_d &= -(i_q - \hat{i}_q)(\omega - \hat{\omega}) - \bar{k}_1(i_d - \hat{i}_d) - \bar{k}_2(i_q - \hat{i}_q) - \bar{k}_3(\omega - \hat{\omega}) + \hat{u}_d, \\ u_q &= (i_d - \hat{i}_d)(\omega - \hat{\omega}) - \bar{k}_4(i_d - \hat{i}_d) - \bar{k}_5(i_q - \hat{i}_q) - \bar{k}_6(\omega - \hat{\omega}) + \hat{u}_q. \end{aligned} \tag{27}$$

To demonstrate the effectiveness of the proposed control laws in (27), the control gains are selected as $\bar{k}_1 = 5$, $\bar{k}_2 = 3$, $\bar{k}_3 = 3$, $\bar{k}_4 = -5$, $\bar{k}_5 = 8$, $\bar{k}_6 = 20$, and the desired angular speed is chosen as follows:

$$\hat{\omega} = \begin{cases} 5 & t < 50 \\ 8 & 50 \le t < 100 \\ 0 & t \ge 100 \end{cases}.$$

The control signals are put into effect when $t \ge 20$ s. The simulation results are depicted in Figure 4. It can be seen from Figure 4 that when the controller is activated, the system states converge to the desired trajectory.

Moreover, when the desired angular speed is designed to follow a sinusoidal or ramp function, the system states

transition immediately from chaotic behavior to the desired trajectory, as illustrated in Figure 5.

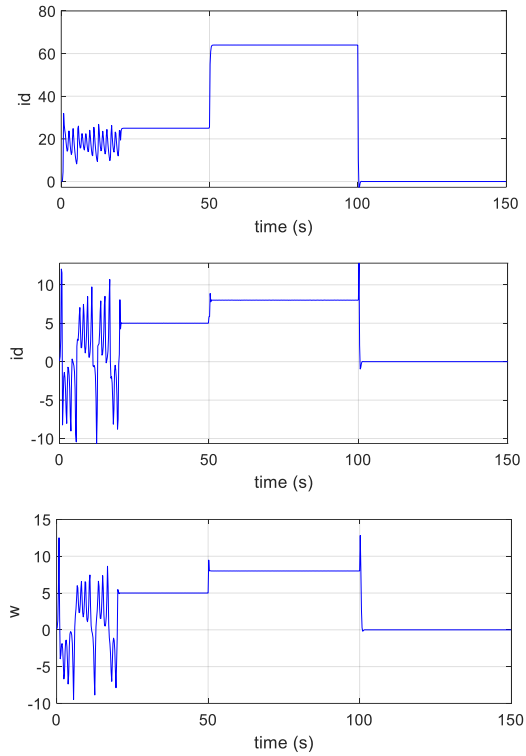

Figure 4. *Time series of the state variables (i_d, i_q, ω), which initially exhibit chaotic oscillations, quickly follow the desired trajectories when the control laws in (27) are applied at t = 20 s*

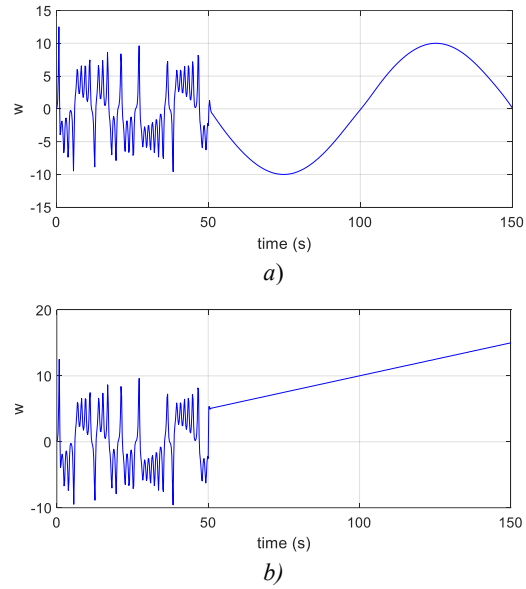

Figure 5. *Time series of the motor's angular speed, which initially exhibit chaotic oscillations, quickly follow a) the desired sinusoidal trajectory, and b) the desired ramp trajectory when the control laws in (27) are applied at t = 20 s*

4. Conclusion

In this study, we addressed the problem of controlling chaos in the PMSM model. A clear picture of chaos in the PMSM model was provided by exploring the Lyapunov exponents and the bifurcation diagram. The appearance of chaos in PMSM machines can lead to serious problems in motion systems driven by PMSM. Therefore, it is essential to suppress unwanted chaotic oscillations through appropriate external control signals. Based on the input-state linearization technique, the control laws for both stabilization and tracking control problems were derived. The numerical simulations demonstrate the effectiveness of the proposed control methods. In addition, the proposed control laws utilize measureable system states to compute the direct and quadrature stator voltage components, which tare used as controlled variables. Therefore, they are straightforward to implement in real applications.

REFERENCES

[1] D.C. Hamill and D.J. Jefferies, "Subharmonics and chaos in a controlled switched-mode power converter", *IEEE Transactions on Circuits and Systems*, vol. 35, no. 8, pp. 1059-1061, 1998. https://doi.org/10.1109/31.1858.

[2] K. Kuroe and S. Hayash, "Analysis of bifurcation in power electronic induction motor drive systems", in *Proceedings of IEEE Power Electronics Specialists Conference, IEEE,* 1989, pp. 923-930. https://doi.org/10.1109/PESC.1989.48578.

[3] J.H. Chen, K.T. Chau, S.M. Siu, and C.C. Chan, "Experimental stabilization of chaos in voltage-mode DC drive system", *IEEE Transactions on Circuits and Systems I: Fundamental Theory and Applications*, vol. 47, no. 7, pp. 1093-1095, 2000. https://doi.org/10.1109/81.855466.

[4] S-C. Chang, "Analytical routes to chaos and controlling chaos in brushless DC motor", *Processes*, vol. 10, no. 5, pp. 814, 2022. https://doi.org/10.3390/pr10050814.

[5] Y. Gao, "Chaotification of induction motor drives under periodic speed command", *Electric Power Components and Systems*, vol. 31, pp. 1083-1099, 2003. https://doi.org/10.1080/15325000390243292.

[6] Y. Gao and K.T. Chau, "Design of permanent magnets to avoid chaos in PM synchronous machines". *IEEE Transactions on Magnetics*, vol. 39, no. 11, pp. 2995-2997, 2003. https://doi.org/10.1109/TMAG.2003.816718.

[7] Y. Gao and K.T. Chau, "Hopf bifurcation and chaos in synchronous relectance motor drives", *IEEE Transactions on Energy Conversion*, vol. 19, no. 2, pp. 296-302, 2004. https://doi.org/10.1109/TEC.2004.827012.

[8] J.H. Chen, K.T. Chau, C.C. Chan, and Q. Jiang, "Subharmonics and chaos in switched reluctance motor drives". *IEEE Power Engineering Review*, vol. 22, no. 2, pp. 57, 2002. https://doi.org/10.1109/MPER.2002.4311981.

[9] Z. Jing, C. Yu, and G. Chen, "Complex dynamics in a permanent-magnet synchronous motor model", *Chaos, Solitons & Fractals*, vol. 22, no. 4, pp. 831-848, 2004. https://doi.org/10.1016/j.chaos.2004.02.054.

[10] L.H. Nguyen, T.D. Le, H.M. Nguyen, and Q.V. Doan, "Control of bifurcation and chaos in the model of the permanent magnet synchronous motor", *The University of Danang - Journal of Science and Technology* –, vol. 11, no. 1, pp. 15-20, 2014.

[11] A. M. Harb, "Nonlinear chaos control in a permanent magnet reluctance machine", *Chaos, Solitons & Fractals*, vol. 19, no. 5, pp. 1217-1224, 2004. https://doi.org/10.1016/S0960-0779(03)00311-4.

[12] Q. Yao *et al.*, "Fixed-time adaptive chaotic control for permanent magnet synchronous motor subject to unknown parameters and perturbations", *Mathematics*, vol. 11, no. 14, pp. 3182, 2023. https://doi.org/10.3390/math11143182.

[13] M. Tahmasbi, "Chaos control in networked permanent magnet synchronous motor using Lyapunov-based model predictive subject to data loss", *Engineering Reports*, vol. 6, no. 5, 2024. https://doi.org/10.1002/eng2.12765.

[14] A. Karimi, H. Akbari, S. Mousavi, and Z. Beheshtipour, "Design of an adaptive terminal sliding mode control to the PMSM chaos phenomenon", *Systems Science & Control Engineering*, vol. 11, no. 1, pp. 1-12, 2023. https://doi.org/10.1080/21642583.2023.2207593.

[15] M. Ataei, A. Kiyoumarsi, and B. Ghorbani, "Control of chaos in permanent magnet synchronous motor by using optimal Lyapunov exponents placement", *Physics Letters A*, vol. 374, no. 41, pp. 4226-4230, 2010. https://doi.org/10.1016/j.physleta.2010.08.047).